IMEKO 24th TC3, 14th TC5, 6th TC16 and 5th TC22 International Conference
11 – 13 October 2022, Cavtat-Dubrovnik, Croatia

UNIVERSAL AUTOMATION APPROACH FOR EFFICIENT CALIBRATION OF ROCKWELL HARDNESS REFERENCE BLOCKS

M. Zackaria[1], F. Menelao[1], D. Nimptsch[2], T. Stegmaier[3], P. Beisel[4], P. Reinstaedt[5], U. Brand[1], R. Tutsch[6]

[1] Physikalisch-Technische Bundesanstalt, Braunschweig, Germany, febo.menelao@ptb.de
[2] Kögel Werkstoff- und Materialprüfsysteme GmbH, Leipzig, Germany, daniel.nimptsch@koegel-leipzig.de
[3] ESI Prüftechnik GmbH, Wendlingen am Neckar, Germany, thomas.stegmaier@esi-prueftechnik.de
[4] KB Prüftechnik GmbH, Hochdorf-Assenheim, Germany, beisel@kbprueftechnik.frm.de
[5] Materialprüfungsamt Nordrhein-Westfalen, Dortmund, Germany, reinstaedt@mpanrw.de
[6] Technische Universität Braunschweig (IPROM), Braunschweig, Germany, r.tutsch@tu-bs.de

Abstract:
Hardness reference blocks play a pivotal role in ensuring traceability of hardness measurements. However, it is challenging to calibrate them in accordance with part three of the ISO 6508 without performing time-consuming pre-measurements. Previously, a method was developed and tested at the PTB for the Rockwell scale HRA which used data from the preload phase to automate the calibration process. We now present a novel method that extends the existing automation method to every standardised Rockwell scale. Furthermore, this method is universal in nature and not restricted to PTB's standardised Rockwell hardness testing machine. Important parameters which pave the way towards the universal automation are addressed. The results of the established characteristic curves are validated by an interlaboratory comparison. This approach accelerates the entire calibration procedure, eliminates the need for an expert user and guarantees a standard-compliant measurement.

Keywords: Rockwell hardness test; standardised testing cycle; automated approach

1. INTRODUCTION

The Rockwell hardness test is unequivocally the most popular method to characterize materials. Industries are heavily reliant upon it for the purposes of material selection, acceptance testing of products and process control. The simplistic definition of hardness based on the indentation depth combined with advantages such as speed of operation, low-cost and a relative non-destructive nature of testing renders it as an indispensable manufacturing tool. From a metrological perspective, the Rockwell scale is empirical in nature. Hence, a strict adherence to the relevant standard is necessary to obtain meaningful and comparable measurement results [1]. This includes defining a standard testing cycle, especially the final speed of indentation. Unfortunately, a world-wide unified Rockwell hardness scale with metrological traceability has not yet been established. This is a major drawback with respect to international trade and global manufacturing [2].

On a national level, hardness reference blocks calibrated by national metrology institutes or accredited testing laboratories are used in the industry for indirect verification and daily verification of Rockwell hardness testing machines [3]. Given its importance, the calibration of these certified hardness reference blocks is standardised in ISO 6508-3 with significantly narrower tolerances than in ISO 6508-1. Nevertheless, the standard does not specify the initial speed of indentation during the application of the additional test force [4]. It has been shown in [5] that this speed is dependent upon the hardness of the material being tested. However, the hardness of the material is a quantity that is to be measured and not something known a priori. Therefore, prior to the automation [5], multiple pre-measurements were necessary to ensure a compliance with the standard. Pre-measurements are tedious, and the overall calibration process requires an expert user, in contrast to the benefits of Rockwell hardness testing.

The focus of this paper is to extend the concept of automation introduced in [5]. The estimation of the initial indentation velocity is redefined. We establish machine-independent characteristic curves for every standardised Rockwell and Superficial Rockwell scale and discuss the techniques to implement it into any other Rockwell hardness testing machine.

2. STANDARD TESTING CYCLE

As described in [4], we begin with the detection of the surface of the hardness reference block with a velocity no more than 1000 μm/s. This is followed by the application of the preliminary force F_0 and a corresponding dwell time. The reference depth h_0 is measured during this step, as shown in Figure 1.

Then, the additional force F_1 is applied in T_{aa} seconds until the total force F is reached. This corresponds to the indentation depth h_2. It must be noted that a constant indentation velocity v_2 is prescribed after 80 % of the total force is reached. We define the indentation velocity prior to this as v_1. The total force is held for a certain amount of time before returning to the preliminary force again. The indentation depth h_1 is measured before separating the indenter from the reference block. The Rockwell hardness value is given by:

$$HR = N - \frac{h}{S} . \tag{1}$$

In Equation (1), N and S are scale dependent constants and h is the difference between h_1 and h_0, as indicated in the Figure 1.

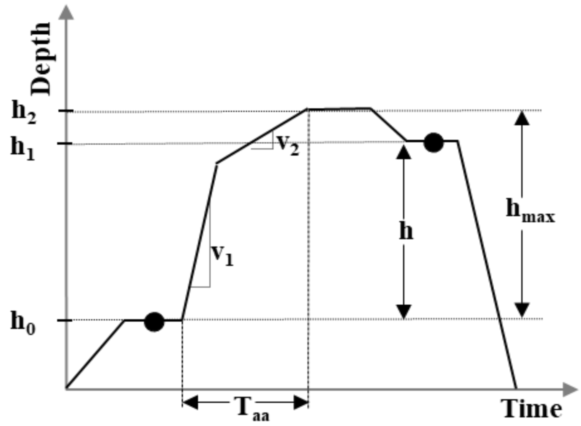

Figure 1: Typical indentation depth vs. time curve

The effect of force application rate during each of the phases of Rockwell hardness test has been described in [1]. Of particular importance is the indentation speed v_2 during the final part of the application of the additional force. When the indentation velocity was varied from 0.5 µm/s up to 70 µm/s, a difference of about 0.6 HRC was observed. Thus, the standard [4] requires a final indentation velocity v_2 between 15 µm/s and 40 µm/s. In an effort to improve the harmonization of primary standards, the working group on hardness (CCM-WGH) of the International Committee for Weights and Measures (CIPM) has agreed upon a final indentation velocity of 15 µm/s for the HR15N scale and 30 µm/s for the HRC, HR30N and HR45N scales.

For the purposes of estimating the initial indentation velocity v_1, characteristic curves are required as shown in [5]. A linear relationship between force and indentation depth was assumed in [5] to obtain the ratio of the indentation depths during the application of the additional test force. However, it has been shown in [6] that the force vs. indentation depth curve can be best described using a power law of the form

$$F = a\,h^b . \tag{2}$$

Here, a and b are constants that depend upon the material and indenter respectively. For self-similar indenters such as Berkovich and Vickers, the constant b is equal to 2 as proved in [7]. Since Rockwell indenters are either spheroconical or spherical in shape, they do not belong to the class of self-similar indenters. Furthermore, the shape of the indenter in contact with the material changes based on the total force and the mechanical properties of the material.

In the case of a spherical indenter, at indentation depths beyond the onset of plasticity, we can decompose the measured indentation depths into elastic and plastic part as shown in [8] as follows:

$$h = h_e + h_p . \tag{3}$$

The elastic indentation depth can be calculated using the Hertzian theory of contact [9]. According to Johnson [10], a material begins to yield when the maximum contact pressure is 1.6 times the yield strength. Combining both elastic and plastic deformations, we get

$$h = \left[\frac{9}{16\,R\,E_r^2}\right]^{1/3} F^{2/3} + \frac{0.058}{R\,\sigma_y} F . \tag{4}$$

In the Equation (4), R is the radius of the indenter and E_r and σ_y are the reduced elastic modulus and the yield stress of the material respectively.

If the indentation depth and the radius of the indenter are of similar magnitude, then the type of deformation would depend upon the material properties. For hard materials, the elastic deformation dominates if the radius of the indenter is much larger than the indentation depth. In general, it can be said that the constant b varies between 1 and 2.

Deriving an analytical relation in the case of a spheroconical Rockwell indenter is not straightforward because of the indentation depth dependent shape of the indenter. Therefore, nonlinear least squares method is used on the available measurement data to find the constants in Equation (2). Table 1 shows the results of the curve fit for three different hardness of steel at maximum loads based on their respective Rockwell scales and for an aluminium and brass hardness reference block each. It is clear from the table that the constant a increases with the increase in the material hardness. Furthermore, the constant b varies between 1 and 2, but is relatively close to 1.5. Combination of a soft material and high load leads to values closer to 2 because the spherical portion of the spheroconical Rockwell indenter can then be neglected.

Table 1: Best fit values of the constants a and b for a power law relationship between force and depth

Nominal Value	Max. Load	*a*	*b*
20 HRC (Steel)	HRA	0.76	1.38
	HRD	0.50	1.48
	HRC	0.30	1.58
40 HRC (Steel)	HRA	1.80	1.29
	HRD	1.24	1.38
	HRC	0.77	1.48
65 HRC (Steel)	HRA	3.75	1.23
	HRD	2.79	1.31
	HRC	2.03	1.38
110 HV (Aluminium)	HRA	0.2	1.55
	HRD	0.14	1.62
35 HRA (Brass)	HRA	0.14	1.56
	HRD	0.10	1.64

We proceed by assuming a value of 1.5 for the constant b. Equation (2) can be rearranged in terms of the indentation depth as:

$$h = \left(\frac{F}{a}\right)^{1/b}. \tag{5}$$

With Equation (5), we can now estimate the percentage of the total indentation depth associated with 80 % of the total force. Let this percent be c. Then, the ratio of the distance traversed by the indenter between 80 % and 100 % of the total load to the total indentation depth during the application of the additional test load is given by:

$$\alpha = (1 - c)\frac{h_2}{h_{\max}}. \tag{6}$$

Expressing Equation (6) in terms of force, we get

$$\alpha = (1 - c)\frac{F^{1/b}}{F^{1/b} - F_0^{1/b}}. \tag{7}$$

With the help of the ratio α, we can calculate the time taken for the final part of the application of the additional force:

$$t_2 = \frac{\alpha\, h_{\max}}{v_2}. \tag{8}$$

Similarly, we can calculate the initial indentation velocity v_1 as

$$v_1 = \frac{[(1 - \alpha)\, h_{\max}]}{[T_{\mathrm{aa}} - t_2]}. \tag{9}$$

In Equation (9), all the variables except $h_{\max}$ are constants and known beforehand. In the next section, we deal with the estimation of $h_{\max}$ based on the measured value of h_0 and the parameters affecting its value.

3. PARAMETER IDENTIFICATION

During the preload phase of a Rockwell hardness test, the indentation depth h_0 is measured. With the help of a database of characteristic curves, the Rockwell hardness value is estimated depending on the measured h_0 value. The next set of characteristic curves estimates $h_{\max}$ based on the Rockwell hardness [5]. Finally, v_1 can be estimated using Equation (9). Figure 2 summarises this general approach of automation.

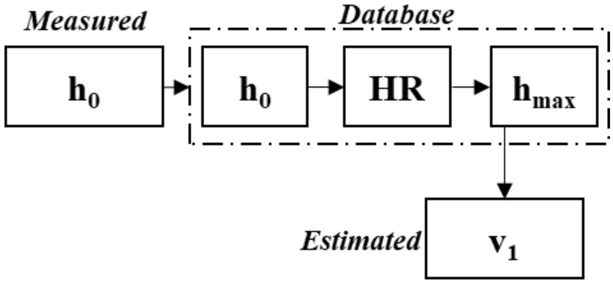

Figure 2: Concept of automation

However, this concept of automation only applies to the testing machine with which the characteristic curves were determined. Thus, one needs to identify the parameters that affect these characteristic curves before implementing it into another hardness testing machine. The critical parameters include, but are not limited to, the surface detection error, the machine compliance, and the velocity corrections. A brief description of these parameters, their significance, and methods to determine them are now discussed.

Surface Detection Error

Typically, when the force signal exceeds a predefined threshold, it is assumed that the surface has been detected. Alternatively, a sudden drop in the indentation velocity indicates the contact between the indenter and the hardness reference block. Both methods perform well for a typical Rockwell hardness test because of the reference depth set at the preload. Since absolute values of $h_{\max}$ and h_0 are required for establishing universal characteristic curves, it is important to address the differences arising from the surface detection. Depending on the force measurement system, an apt threshold must be chosen. The finite deformation (Δx) that occurs until the force threshold is reached can be calculated using the Equation (4).

Machine Compliance

In the framework of the automation, the machine compliance plays a crucial role. The measured displacement in any hardness testing machine comprises not only the indentation depth, but also the deformation of the machine frame itself. The extent of this elastic deformation depends significantly on the machine design. Observations have shown that a typical C-frame hardness testing machine could deform in the range of hundreds of micrometres during Rockwell tests. To measure the compliance, the method described in [11] works well. Here, it is assumed that the machine frame and the contact between the material and the indenter work as two springs in series. Performing hardness measurements for three scales such as HRA, HRD and HRC on the same material and analysing the slopes of the unloading curves gives us the total measured compliance C_t for each indentation. The Sneddon's equation of contact stiffness between the material and the indenter [12] is then rearranged in terms of the maximum applied force F_{max} and it is assumed that the hardness and reduced elastic modulus are constants over the entire depth of indentation as shown in Equation (10). This is a linear equation, and the y-intercept of this curve gives us the machine compliance C_{f}. Figure 3 visualises the force-depth curves of three indents after the machine compliance has been subtracted from the measured indentation depth. The statistical results of the measured machine compliance are very consistent, and the choice of material and material hardness did not seem to affect the results significantly.

$$C_t = \frac{k}{\sqrt{F_{max}}} + C_f \,. \tag{10}$$

The corrected $h_{\max}$ and h_0 are then given by Equation (11) and Equation (12) respectively

$$h_{\max} = h_{\max\,(\text{measured})} - F\,C_{\mathrm{f}} \,. \tag{11}$$

$$h_0 = h_{0\,(\text{measured})} - F_0\,C_{\mathrm{f}} + \Delta x \,. \tag{12}$$

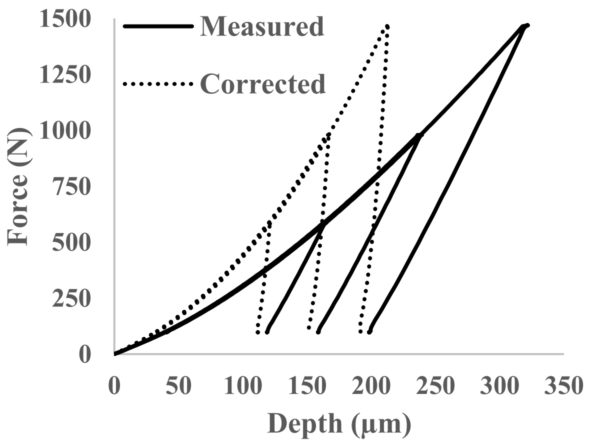

Figure 3: Load-displacement curves (HRA, HRD and HRC) before and after machine compliance correction

Velocity Corrections

Depending on the hardness of the reference block, the input or the estimated velocity differs from the actual or measured velocity during the indentation process. It can be seen in Figure 4 that this difference exists both for v_1 and v_2. Furthermore, this effect is much more profound for softer materials in case of v_1. As for v_2, the measured velocity is greater than the set velocity for softer materials and smaller for harder materials. Since, high reproducibility and repeatability of the actual indentation velocity is required to adhere to the standard, velocity correction factors are needed. These velocity correction factors manipulate the speed of the motor based on the estimated initial velocity v_1. To determine these correction factors, the input velocity is incremented for every available hardness value, and the corresponding output velocity is measured. This is performed for both v_1 and v_2, because the range of the theoretical indentation depth is totally different for each of the velocities.

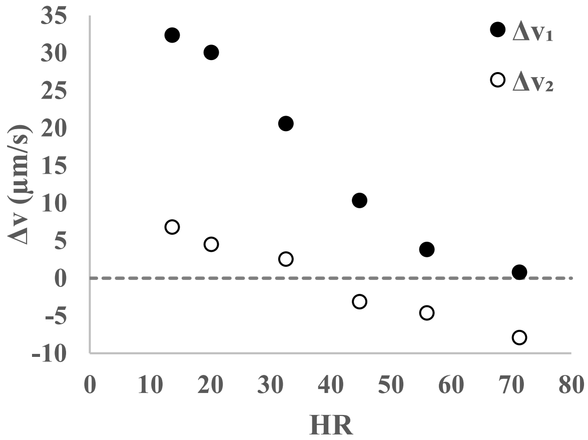

Figure 4: Variation of the difference between the measured and set velocity over the measured hardness

As shown in Figure 5, the output to input ratio for both v_1 and v_2 varies linearly with the hardness value. The results of different sets of output and input velocities for each hardness value have been indicated with the corresponding trendlines. With the help of the estimated hardness value during the preload phase, the necessary velocity correction factors can be calculated, and the motor speed adjusted accordingly.

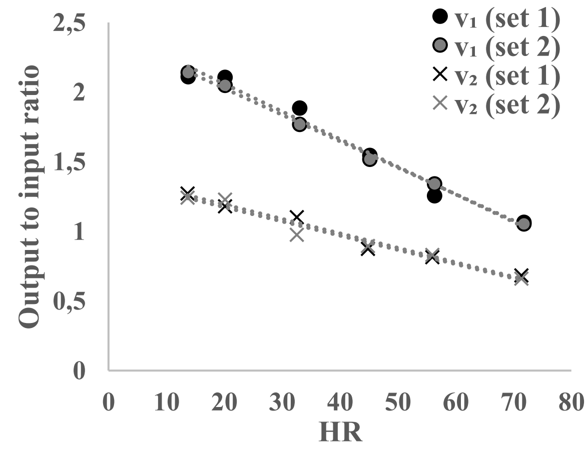

Figure 5: Linear relationship of the output to input ratio of velocities with respect to the measured hardness

4. VALIDATION AND DISCUSSION

Based on the concept of automation and the determined parameters, an interlaboratory comparison has been carried out to test the feasibility of the method. For the purposes of anonymity, they are represented as Lab A and Lab B. A force threshold of 0.5 N was agreed upon for the purposes of surface detection. The machine compliance of Lab A and Lab B were calculated to be 75 nm/N and 9.8 nm/N respectively. A total of 15 different nominal hardness values and 3 industry typical materials brass, aluminium and steel were used for the analysis. For each of the data points, 10 indents were performed to obtain a good statistical representation of the relationship. Finally, all of this was performed for every standardised Rockwell hardness scale. The following results are an extract from the database of steel being tested using an HRC scale.

The results of the estimation of the hardness value HRC based on h_0 for Lab A and Lab B are shown in the Figure 6. After consideration of the surface detection and the machine compliance, the machine-independent characteristic curves are shown in Figure 7.

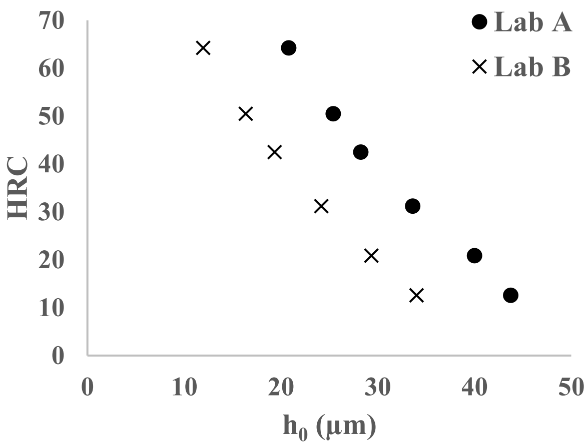

Figure 6: Machine-dependent characteristic curves (I)

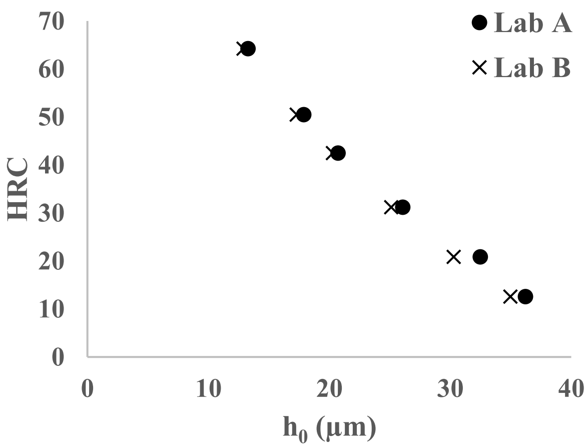

Figure 7: Machine-independent characteristic curves (I)

A logarithmic function best describes this characteristic curve. However, for the scales that use spherical indenters, a linear fit is more suitable.

Similarly, the estimation of $h_{\max}$ based on the estimated hardness value for machine-dependent and machine-independent databases are shown below in Figure 8 and Figure 9 respectively. For every scale, a linear function best describes these characteristic curves.

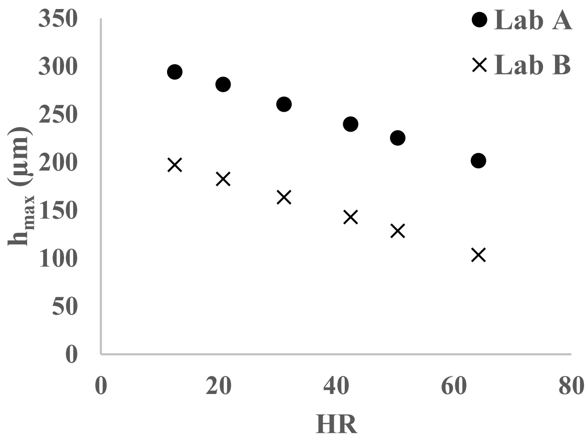

Figure 8: Machine-dependent characteristic curves (II)

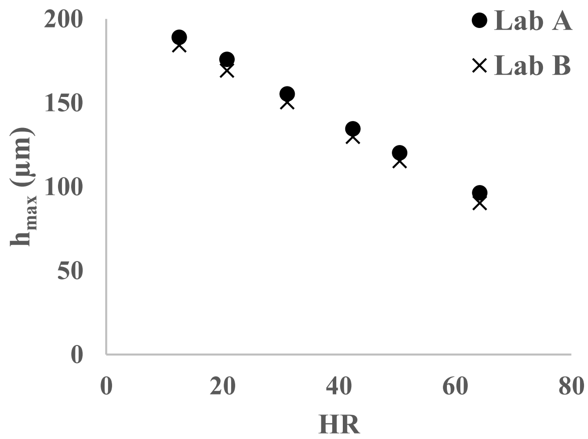

Figure 9: Machine-independent characteristic curves (II)

It can safely be said that there is a good agreement between the results determined by two totally different Rockwell hardness testing machines. The minor differences can be attributed to the fact that different indenters were used to establish the characteristic curves. As mentioned in [1], indenter geometry is the dominant uncertainty source in a Rockwell hardness test. Furthermore, although the hardness reference blocks had the same nominal hardness values, the true hardnesses were not the same.

It must also be mentioned that for Rockwell hardness scales that use a spherical indenter, especially the HR15T scale, the measured hardness is extremely sensitive to the indentation velocity. This represents a different kind of challenge in establishing the characteristic curves because the relation between h_0, $h_{\max}$ and HR changes with every change in the indentation velocity. This effect is compounded due to the low total test force of the HR15T scale and the use of a tungsten carbide spherical indenter rather than a diamond indenter.

Also, parameters such as indenter geometry, load calibration and depth calibration, etc. have not been considered in this study. Surface roughness of the hardness reference blocks could also affect the database of characteristic curves. However, we assume that the hardness reference blocks do not have a roughness value of R_a greater than 0.3 µm as required by the ISO standard. In some cases, an overshooting can occur due to the magnitude of the final velocity v_2. This can be suppressed by programming a third velocity after 99 % of the total force is reached. This additional velocity does not contradict the requirements of the standard.

It has also been shown that assuming a linear relation between the force and indentation depth is not ideal. Although the change of velocity is done based on a force sensor, it would be sensible to see the impact it has based on indentation depth readings. A linear relationship means that b is equal to 1 in Equation (5). Thus, the change of velocity occurs at 80 % of the maximum depth (h_2). On the other hand, if b is equal to 2, the change of velocity occurs at 89 % of h_2. For b equal to 1.5, the change of velocity occurs at 86 %. This error leads to an initial indentation velocity v_1 being maintained for a longer time than stipulated. Therefore, the final velocity v_2 would either exceed or fall behind the set value based on the estimated initial indentation velocity v_1.

Finally, it has been shown in Figure 10 that after the implementation of the presented technique the requirements of the standard are met and a constant final indentation speed of (27 ± 1) µm/s is achieved throughout the HRC scale.

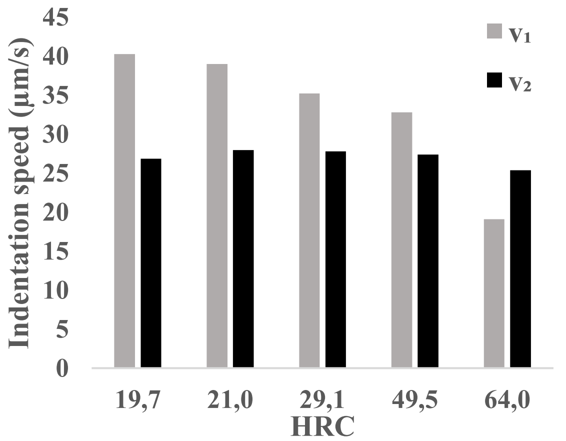

Figure 10: Measured indentation speeds for different hardness values

5. SUMMARY

A universal automated approach to perform calibrations of Rockwell hardness reference blocks has been presented. The interlaboratory comparison of results proved that this technique can be implemented on any computerized Rockwell hardness testing machine. Important parameters that affect the universal characteristic curves were identified and methods to determine them were suggested. It has also been shown that this calibration approach is user-friendly, saves time and cost and most importantly takes a step towards a unified worldwide Rockwell hardness scale. Future work should focus on improving the HR15T characteristic curves and determining indenter geometry correction factors.

6. REFERENCES

[1] S. R. Low, Rockwell Hardness Measurement of Metallic Materials, NIST Recommended Practice Guide, Special Publication 960-5, January 2001. Online [Accessed 20221209] https://www.nist.gov/publications/nist-recommended-practice-guide-rockwell-hardness-measurement-metallic-materials

[2] J.-F. Song, S. Low, D. Pitchure, A. Germak, S. DeSogus, T. Polzin, H.-Q. Yang, H Ishida, G. Barbato, Establishing a world-wide unified Rockwell hardness scale with metrological traceability, Metrologia **34** 331, 1997 DOI 10.1088/0026-1394/34/4/6

[3] DIN EN ISO 6508:2015-2 Metallic materials - Rockwell hardness test - Part 2: Verification and calibration of testing machines and indenters

[4] DIN EN ISO 6508:2015-3 Metallic materials - Rockwell hardness test - Part 3: Calibration of reference blocks

[5] D. Grziwotz, U. Brand, F. Menelao, M. Schilling, Automation of the Rockwell standard measuring machine of the PTB, Int. IMEKO TC5 Conference, Helsinki, Finland, 30 May - 01 June 2017. Online [Accessed 20221209] https://www.imeko.org/publications/tc5-2017/IMEKO-TC5-2017-002.pdf

[6] J. L. Loubet, J. M. Georges, J. Meille, in Microindentation techniques in Materials Science and Engineering, edited by P. J. Blau and B. R. Lawn, American Society for Testing and Materials, pp. 72-89, 1986

[7] S. V. Hainsworth, H. W. Chandler, T. F. Page, Analysis of nanoindentation load-displacement loading curves, Journal of Materials Research, Vol. 11, No. 8, 1996, pp. 1987 - 1995. DOI: 10.1557/JMR.1996.0250

[8] U. Brand, E. Beckert, A. Beutler, G. Dai, Chr. Stelzer, A. Hertwig, P. Klapetek, J. Koglin, R. Thelen, R. Tutsch, Comparison of optical and tactile layer thickness measurements of polymers and metals on silicon or SiO2, Measurement

Science and Technology **22** 094021, 2011. DOI: 10.1088/0957-0233/22/9/094021
[9] H. Hertz, Ueber die Beruehrung fester elastischer Koerper, Journal fuer die reine und angewandte Mathematik **92** 156-171, 1881
[10] K. L. Johnson, Contact Mechanics, Cambridge University Press, 1985
[11] DIN EN ISO 14577-1:2015, Metallic materials – Instrumented indentation test for hardness and materials parameters – Part 1: Test method
[12] I. A. Sneddon, The relation between load and penetration in the axisymmetric boussinesq problem for a punch of arbitrary profile, International Journal of Engineering Science, Vol. 3, Issue 1, 1965, May 1965, pp. 47-57. DOI: 10.1016/0020-7225(65)90019-4